Journal of Solid State Chemistry 184 (2011) 3066–3073

Contents lists available at SciVerse ScienceDirect

Journal of Solid State Chemistry

journal homepage: www.elsevier.com/locate/jssc

ESR study on the visible photocatalytic mechanism of nitrogen-doped novel TiO_2 Synergistic effect of two kinds of oxygen vacancies

Jiwei Zhang, Zhensheng Jin*, Caixia Feng, Laigui Yu, Jingwei Zhang, Zhijun Zhang*

Laboratory of Special Functional Materials, Henan University, Kaifeng 475004, PR China

ARTICLE INFO

Article history:
Received 21 April 2011
Received in revised form
23 July 2011
Accepted 14 September 2011
Available online 22 September 2011

Keywords:
N-doped novel TiO_2
Visible photocatalytic activity
Oxygen vacancy
Synergistic effect
ESR

ABSTRACT

The visible photocatalytic mechanism of nitrogen-doped novel TiO_2 was studied by means of electron spin resonance spectroscopy (ESR). It was found that, under visible light irradiation, the concentration of single-electron-trapped oxygen vacancy (SETOV, $V_o^{\bullet}$) of novel TiO_2 remained unchanged, but that of nitrogen-doped novel TiO_2 increased and returned to original state when the light was turned off. This implies that, aside from $V_o^{\bullet}$ in bulk of nitrogen-doped novel TiO_2, oxygen vacancy without trapped electron ($V_o^{\bullet\bullet}$) was formed on its surface. $V_o^{\bullet\bullet}$ as a surface electron trap captured photogenerated electron from the bulk to generate extra $V_o^{\bullet}$, carrying out photocatalytic reaction on the surface. At the same time, nitrogen doping product NO was chemically adsorbed on the vicinity of $V_o^{\bullet\bullet}$ and inhibited the attack of oxygen, allowing $V_o^{\bullet\bullet}$ to remain stable in air. The synergistic action of the two kinds of active structures, i.e., bulk $V_o^{\bullet}$–NO–Ti and surface $V_o^{\bullet\bullet}$–NO–Ti, accounted for the visible photocatalytic activity of N-doped novel TiO_2.

1. Introduction

Heterogeneous photocatalysis involves an initial stage where semiconductor catalysts are excited by photons to generate high energy electron–hole pairs (e^-–h^+). Semiconductors adsorb light up to a certain depth (for example, TiO_2 adsorbs ultraviolet (UV) light to a depth of about 1 μm) [1,2]. The photogenerated e^-–h^+ pairs in the bulk must be separated and transferred to surface and captured by surface traps; otherwise, redox reactions of adsorbed reactants cannot take place thereon. It is well known that only those surface traps with energy level lower than the conduction band edge of semiconductors can play the role of electron traps (see Scheme 1) [3–5].

Surface traps of photogenerated electrons can be formed either during light irradiation or during preparation. The band gap (E_g) of anatase TiO_2, i.e., the energy difference between the lowest unoccupied molecular orbit (LUMO) of Ti3d and the highest occupied molecular orbit (HOMO) of O2p, is 3.2 eV. Under ultraviolet irradiation, Ti^{4+}–O^{2-} on the surface of TiO_2 will be transformed to Ti^{3+}–O^-. According to Frank–Condon principle, such a variation of valences requires rearrangement of ions on the surface to form active sites. The energy level of the active sites falls between the unoccupied energy level and occupied one plus the difference of relocation energy for the two types of oxidation states [6]. By doping with metal ions, TiO_2 can be endowed with visible light response. Unfortunately, metal-doped TiO_2 cannot produce surface electron traps originated from Frank-Condon effect under visible light irradiation, showing no visible light catalytic activity [7,8]. At the same time, a special preparation technique is imperative for generating surface traps.

According to He atomic model, oxygen vacancy in TiO_2 can be classified into three categories [9]: double-electron-trapped oxygen vacancy (denoted as $V_o^{\times}$, effective charge 0), single-electron-trapped oxygen vacancy (denoted as $V_o^{\bullet}$, effective charge +1) and oxygen vacancy without trapped electron (denoted as $V_o^{\bullet\bullet}$, effective charge +2). Of the three kinds of oxygen vacancies, only $V_o^{\bullet}$ contributes to ESR signal (g=2.004) [9–12]. As reported by Croneemeyer [9], the first ionization energy (E_1) of $V_o^{\times}$ is 0.75 eV (upward towards the bottom of conduction band) and second ionization energy (E_2) 1.18 eV. E_1 can be moved towards the conduction band with the increase of the concentration of oxygen vacancy (N_d). When N_d is above 1.9×10^{25} (spin/m^3), E_1 is immersed in the conduction band. In this case, only E_2 (corresponds to the energy level of $V_o^{\bullet}/V_o^{\bullet\bullet}$) remains in the E_g of TiO_2; and the g factor of electrons trapped in the oxygen vacancies ($V_o^{\bullet}$) of TiO_2 converges to that of free electrons (g=2.0036).

What should be emphasized is that the origin of visible photocatalytic activity of N-doped TiO_2 still remains disputable. Some researchers suggested that valence band was consisted of $^{\bullet}$N directly, or from overlapping of N2p orbital with O1s orbit

* Corresponding authors. Fax: +86 378 3881358.
E-mail address: jinzhensheng@henu.edu.cn (Z. Jin).

0022-4596/$ - see front matter © 2011 Elsevier Inc. All rights reserved.
doi:10.1016/j.jssc.2011.09.016

occurred in N-doped TiO_2, resulting in band gap narrowing and visible photocatalytic activity [13–16]. This viewpoint, however, was argued by Serpone et al. who supposed that the visible light photocatalytic activity of N-doped TiO_2 is related to the generation of color centers [17–19]. In connection with our previous investigation of N-doped novel TiO_2 [20–23], we also argued against the band-gap-narrowing viewpoint.

We obtained a novel TiO_2 (anatase) by dehydration of nanotube titanic acid (NTA) at elevated temperature in air [24]:

$$H_2Ti_2O_4(OH)_2 \rightarrow 2TiO_{2-x}(V_o^{\bullet})_x + yH_2O \quad (1)$$

The novel TiO_2 contains high concentration of single-electron-trapped oxygen vacancies ($V_o^{\bullet}$) which are able to form a sub-band within the band gap, resulting in a strong visible light response [24–28]. However, the novel TiO_2 is inert under visible light irradiation. After the novel TiO_2 was calcinated in NH_3 flow at elevated temperatures, resultant N-doped novel TiO_2 had unchanged crystalline form and visible light absorption property, but it showed visible photocatalytic activity. We suggested that NO chemically adsorbs on the vicinity of $V_o^{\bullet}$ in bulk and inhibits the emission of fluorescence resulted from trapped exciton ($V_o^{\bullet}$–h^+) recombination, favoring the transfer of photogenerated electrons to its surface and resulting in visible photocatalytic activity [20–23]. Recently, based on electron spin resonance (ESR) analysis, we found that, under visible light irradiation, the concentration of $V_o^{\bullet}$ contained in the novel TiO_2 keeps unchanged, but that in the N-doped novel TiO_2 increases and returns to original state upon turning off light. This reminds us that we still have a spare room to modify our viewpoint about the origin of visible photocatalytic activity of the N-doped novel TiO_2 [22].

2. Experimental

2.1. Preparation of photocatalysts

Synthesis of nanotube titanic acid (NTA) was reported elsewhere (see Fig. 1a) [29–31]. Briefly, the preparing procedure of NTA is as follows: P25–TiO_2 reacted with 10 M concentrated NaOH solutions at 120 °C for 24 h to obtain nanotube $Na_2Ti_2O_5 \cdot H_2O$. Then the precipitates were rinsed with distilled water until pH=10, then put into 0.1 M HCl solution for 5 h. Afterward, the precipitates were washed with distilled water until pH close to 7, and dried at 120 °C. When NTA is heated above 300 °C, it is converted from orthorhombic to anatase (Fig. 2) *via* dehydration. The so-called novel TiO_2 was prepared by dehydrating NTA at 600 °C in air for 2 h (see Fig. 1b). A certain amount of novel TiO_2 was put in a small quartz boat and heated at 600 °C for 4 h in a tubular furnace under NH_3 (purity 99.9%) gas flow. After being cooled to room temperature in NH_3 gas flow, N-doped novel TiO_2 was obtained (see Fig.1c) and it was stored in a desiccator.

2.2. Characterization

A Brüker ESP300E apparatus was performed to record the ESR spectra at a microwave frequency of 9.80 GHz, microwave power of 10 mW, modulation frequency of 100 kHz, modulation amplitude of 2 G and scanning time of 41.9 s. The same quartz capillary tube with an inner diameter of about 1 mm was used for ESR measurements at a fixed sample height. The ESR data were calibrated in relation to $g=2.0036$ of diphenyl picryl hydrazyl (DPPH). A laser of 532 nm was used as the light source for illumination test. X-ray diffraction patterns (XRD) were obtained with a Philips X'Pert Pro X-ray diffractometer. An ESCALAB210 X-ray photoelectron spectroscope (XPS) was used to determine surface composition and valence state, and the binding energy of contaminant carbon (C 1*s*: 284.8 eV) was adopted to calibrate XPS data. Diffuse reflectance spectra (DRS) were measured with a Shimadzu U-3010 spectrometer. Photoluminescence spectra (PL) were measured with an SPEXF212 spectrometer (slit=4).

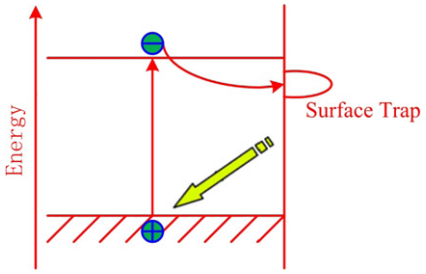

Scheme 1. Surface electron trap.

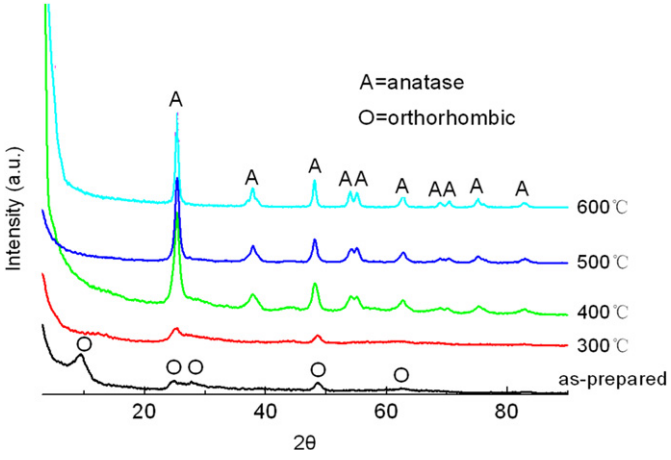

Fig. 2. XRD patterns of NTA dehydrated at different temperatures in air.

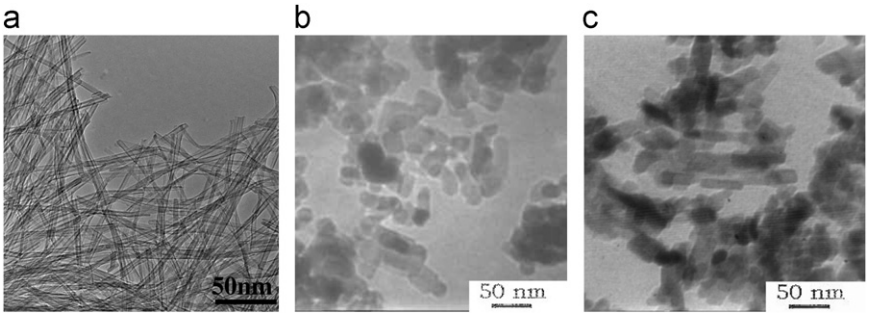

Fig. 1. TEM images of (a) NTA, (b) novel TiO_2 (anatase) and (c) N-doped novel TiO_2 (anatase).

2.3. Evaluation of photocatalytic activity

The photocatalytic activity of catalysts was evaluated by monitoring the photocatalytic oxidation reaction of propylene. 31 ± 1 mg of catalyst sample was dispersed in 10 mL of distilled water and spread on the roughened surface of a glass plate (0.9 cm × 11 cm × 0.2 cm). The glass plate was then put into a flat quartz tube reactor with a dead space of 14 mL. A 500 W xenon lamp was used as the visible light source. Between the xenon lamp and reactor were inserted a cut filter ($\lambda \geq 420$ nm) and a water cell to eliminate ultraviolet and infrared light, outputting visible light ($\lambda \geq 420$ nm) with an intensity of about 1.9 mW/cm^2. A black-light lamp (4 W, main wavelength 365 nm) was used as the ultraviolet source which was irradiated onto the surface of to-be-tested samples at an intensity of 2.5 mW/cm^2 . The mixed gas of C_3H_6 (99.99%) and dry air (concentration of C_3H_6=600 ppmV) was used as the feed gas. The concentration of C_3H_6, C, was determined at a sensitivity of 1 ppmV by using a gas chromatograph (Shimadzu GC-9A) equipped with a flame ionization detector (FID), a GDX-502 column, and a reactor loaded with Ni catalyst for the methanization of CO_2. The removal rate of C_3H_6 was calculated as $(C_0-C)/C_0 \times 100\%$; where C_0 refers to the initial concentration of C_3H_6.

3. Results and discussion

3.1. Physi-chemical properties and photocatalytic activities for different light sources

Fig. 3 shows the XRD and DRS patterns of novel TiO_2 and N-doped novel TiO_2. In terms of crystal form, both novel TiO_2 and N-doped novel TiO_2 belong to anatase (see Fig. 3a). Corresponding XPS datum confirms that N has been successfully doped into novel TiO_2 (see the inset of N 1*s* XPS spectrum in Fig. 3a). Besides, as shown in Fig. 3b, both novel TiO_2 and N-doped novel TiO_2 had a strong response to visible light.

The ESR spectra of the dehydrated products of NTA at different temperatures (T) are shown in Fig. 4a. P25–TiO_2 and as-prepared NTA show no ESR signal. After dehydration of NTA at 100, 200 and 300 °C, resultant dehydrated products (samples B, C and D) have symmetrical ESR peaks with g=2.004 which can be assigned to $V_o^{\bullet}$ [9–12]. The dehydrated products of NTA at increased temperatures of 400 °C, 500 °C and 600 °C (samples E, F and G) show asymmetrical ESR peaks, due to the strong interaction between $V_o^{\bullet}$ [24–26]; and the concentration of $V_o^{\bullet}$ greatly increases owing to the transformation from orthorhombic NTA to anatase TiO_2. Besides, N-doped novel TiO_2, obtained by calcinating sample G (novel TiO_2) in flowing NH_3 at 600 °C for 4 h, shows a triplet ESR signal consisting of one main peak (g=2.004) and two weak peaks (Fig. 4b), which may be attributed to the modification effect of chemisorbed NO and the effect of crystal field on $V_o^{\bullet}$ [22]. Serwicka et al. reported [10] that reduced TiO_2 showed similar triplet ESR signal after adsorbing $C_6H_5NO_2$ at room temperature in vacuum, which was assigned to a superimposition peak of $V_o^{\bullet}$ with $C_6H_5NO_2^-$.

Using $VOSO_4$ as an ESR standard [10], we determined that the $V_o^{\bullet}$ concentration of novel TiO_2 (obtained by dehydration of NTA at 400 °C in air for 4 h) and N-doped novel TiO_2 (obtained by calcination of novel TiO_2 in NH_3 flow at 400 °C for 4 h) is about 1.2×10^{25} (spin/m^3) and 7.4×10^{24} (spin/m^3), respectively ($V_o^{\bullet\bullet}$ may also exist but it cannot be detected by ESR). A high concentration of $V_o^{\bullet}$ should form a sub-band within E_g of TiO_2 [27,28]. Resultant sub-band as a "bridge" can carry the transfer of valence band electrons of TiO_2 to conduction band with the assistance of two visible photons. N-doped novel TiO_2 possesses visible photocatalytic activity for the oxidation of propylene (see Fig. 5a), however, as shown in Fig. 5a, novel TiO_2 is inert under visible light irradiation. It was supposed that the photogenerated charges of novel TiO_2 under visible light irradiation will all disappear by recombination of a trapped electron in an oxygen vacancy with a hole ($V_o^{\bullet}$–h^+) to emit fluorescence, while NO will inhibit the emission of fluorescence and result in visible photocatalytic activity of N-doped novel TiO_2 (see weakened PL spectrum of N-doped novel TiO_2 in Fig. 5d) [22], if so, novel TiO_2 should still remain inert under UV irradiation. But Fig. 5b shows that novel TiO_2 has an UV photocatalytic activity close to that of N-doped novel TiO_2. That is why? This problem was solved by following ESR investigation.

3.2. ESR property of novel TiO_2 (anatase)

Fig. 6a shows the dependence of ESR peak height (h_{SETOV}, proportional to the concentration of $V_o^{\bullet}$) of novel TiO_2 (anatase) on visible-light irradiation time (t). It is seen that h_{SETOV} keeps unchanged with varying t, which hints that $V_o^{\bullet}$ exists only in the bulk. In other words, under visible light irradiation, the sub-band electrons of novel TiO_2 (anatase) were initially excited to conduction band, which was followed by the excitation of valence band electrons to the sub-band forming trapped excitons ($V_o^{\bullet}$–h^+). Simultaneously, the $V_o^{\bullet}$–h^+ were annihilated to form luminescence, accompanied by radiationless return of the conduction band electrons to the sub-band. Since the electron transitions in the bulk of TiO_2 are very fast, it is not possible to detect the transient change in the concentration of $V_o^{\bullet}$ with a Brüker ESP300E apparatus; subsequently, an unchanged concentration of $V_o^{\bullet}$ is observed (Fig. 6a, b). If there were only electron

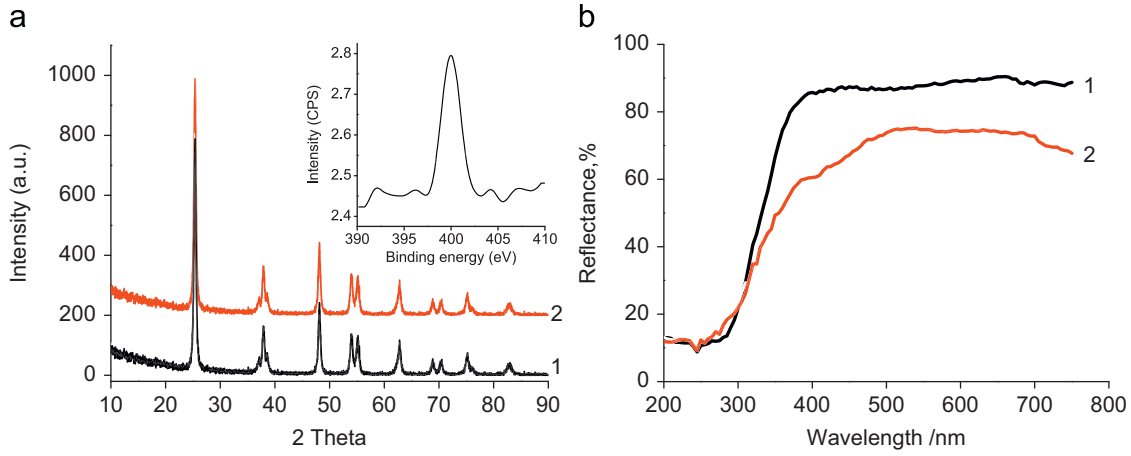

Fig. 3. XRD patterns (a) and DRS spectra (b) of 1-novel TiO_2 (anatase) and 2-N-doped novel TiO_2 (anatase). Inset in left figure is the N 1s XPS spectrum of N-doped novel TiO_2 .

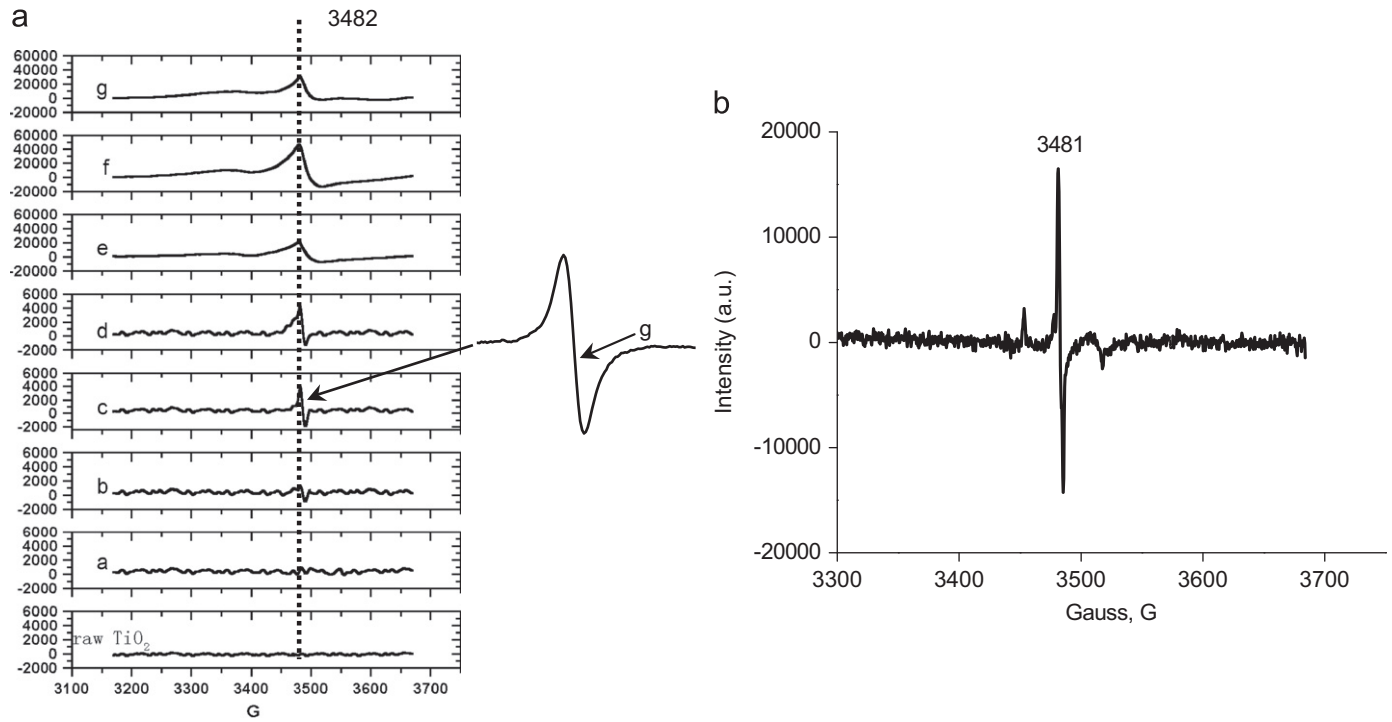

Fig. 4. ESR spectra of (a) (raw TiO_2 Degussa P25; a=as-prepared NTA; b=NTA, 100 °C—2 h; c=NTA, 200 °C—2 h; d=NTA, 300 °C—2 h; e=NTA, 400 °C—2 h; f=NTA, 500 °C—2 h; g=NTA, 600 °C—2 h) and (b) N-doped novel TiO_2 (g=2.003).

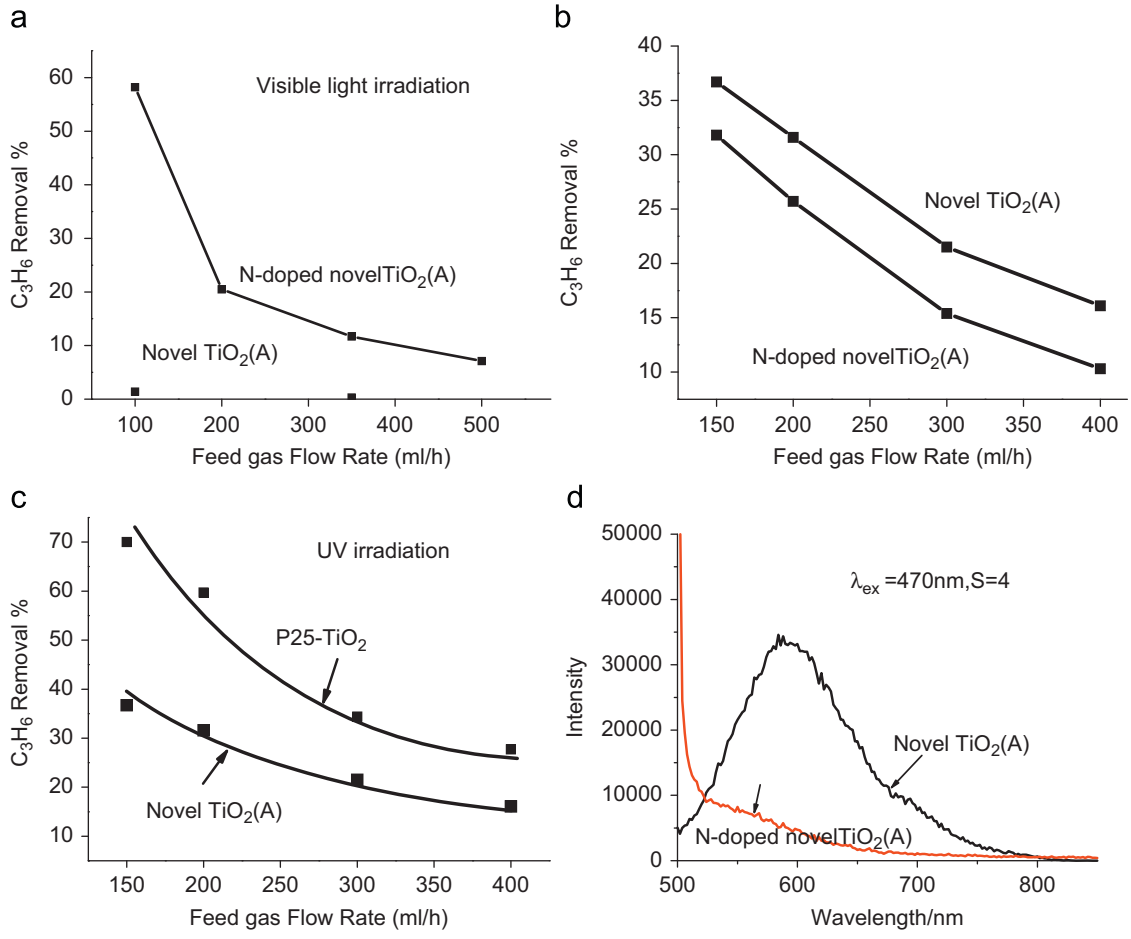

Fig. 5. (a) Visible photocatalytic activity of novel TiO_2 (anatase) and N–doped novel TiO_2 (anatase), (b) UV photocatalytic activity of novel TiO_2 (anatase) and N-doped novel TiO_2 (anatase), (c) UV photocatalytic activity of P25–TiO_2 and novel TiO_2 (anatase) and (d) Photoluminescence spectra of novel TiO_2 (anatase) and N-doped TiO_2 (anatase).

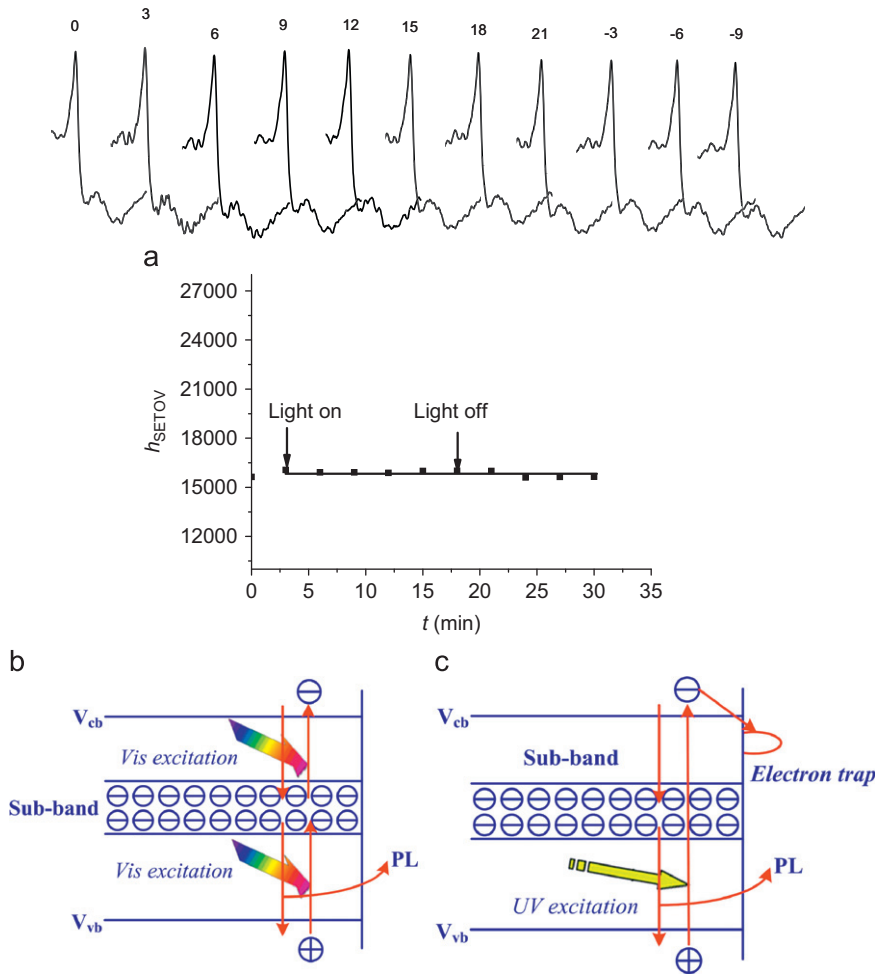

Fig. 6. (a) Dependence of h_{SETOV} of novel TiO_2 (anatase) with irradiation time t under visible light illumination, (b) band structure of novel TiO_2 (anatase) under visible light illumination and (c) band structure of novel TiO_2 (anatase) under UV illumination.

transition between sub-band and conduction band (or between sub-band and valence band) of novel TiO_2, the concentration of $V_o^{\bullet}$ would tend to decrease, because of no ESR signal for $V_o^{\bullet\bullet}$ and $V_o^{\times}$.

Novel TiO_2 (anatase) is a dehydration product of NTA at elevated temperature in air, so it has intact surface structure (see schematic diagram Fig.7a). The lattice structures for the surface layer and bulk of novel TiO_2 can be well distinguished by means of high resolution transmission electron microscopy (HRTEM; see Fig. 7b). Under visible light irradiation, surface electron traps cannot be generated on novel TiO_2 (anatase) [6], and visible photogenerated charges cannot be transferred from the bulk to the surface to conduct redox reactions, thus novel TiO_2 (anatase) becomes inert (Fig. 5a). However, under UV irradiation, electron traps are generated on the surface of novel TiO_2 (anatase) following Frank–Condon principle, resulting in UV photocatalytic activity (see Fig. 5b), even if its UV photocatalytic activity is only about a half of that of P25-TiO_2, due to the simultaneous emission of fluorescence (see Figs. 5c and 6c).

3.3. ESR property of N-doped novel TiO_2 (A)

Fig. 8 shows the dependence of h_{SETOV} of N-doped novel TiO_2 (anatase) on irradiation time. Different from that shown in Fig. 6a, in Fig. 8 h_{SETOV} initially rises and then tends to stabilize at a certain time, followed by returning to original state upon light cut off. This implies that extra $V_o^{\bullet}$ had been generated during the visible-light irradiation of N-doped novel TiO_2 (anatase).

As mentioned earlier, novel TiO_2 under visible-light irradiation retained unchanged $V_o^{\bullet}$ concentration within sub-band. The generation of extra $V_o^{\bullet}$ cannot be detected by ESR unless the following two conditions are simultaneously satisfied. Namely, $(V_o^{\bullet\bullet})_{surf}$ should exist on the surface, by which the photogenerated electrons (e_{cb}^-) can be captured to form $(V_o^{\bullet})_{surf}$ (formula (2)); and at the same time, $(V_o^{\bullet})_{surf}$ should be recombined with h_{vb}^+ (formula (3)) at a rate less than its formation rate (formula (2)). Fig. 8 implies that above two conditions are present simultaneously for N-doped novel TiO_2 (anatase). Under steady state, the concentration ratio of $(V_o^{\bullet})_{bulk}$ to $(V_o^{\bullet})_{surf}$ is equal to 4.6 : 1, corresponding to an increase of $V_o^{\bullet}$ concentration by about 20%. In combination with the results shown in Fig. 5, we believe that modifications should be made from the following two aspects to clarify our viewpoint about the origin of visible photocatalytic activity of N-doped novel TiO_2 (anatase) [22]. First, photogenerated electron e_{cb}^- captured by the surface trap $(V_o^{\bullet\bullet})_{surf}$ of N-doped novel TiO_2 (anatase) allows the photocatalytic reaction of C_3H_6 to be initiated thereon (formulae 4 and 5). The visible photocatalytic activity is attributed to the synergistic effect of $(V_o^{\bullet})_{bulk}$ and $(V_o^{\bullet\bullet})_{surf}$.

$$(V_o^{\bullet\bullet})_{surf} + e_{cb}^- \rightarrow (V_o^{\bullet})_{surf} \quad (2)$$

$$(V_o^{\bullet})_{surf} + h_{vb}^+ \rightarrow (V_o^{\bullet\bullet})_{surf} \quad (3)$$

$$(V_o^{\bullet})_{surf} + O_2 \rightarrow O^{2-} + (V_o^{\bullet\bullet})_{surf} \quad (4)$$

$$O^{2-} + C_3H_6 + h_{vb}^+ \rightarrow \text{Oxidized products} \quad (5)$$

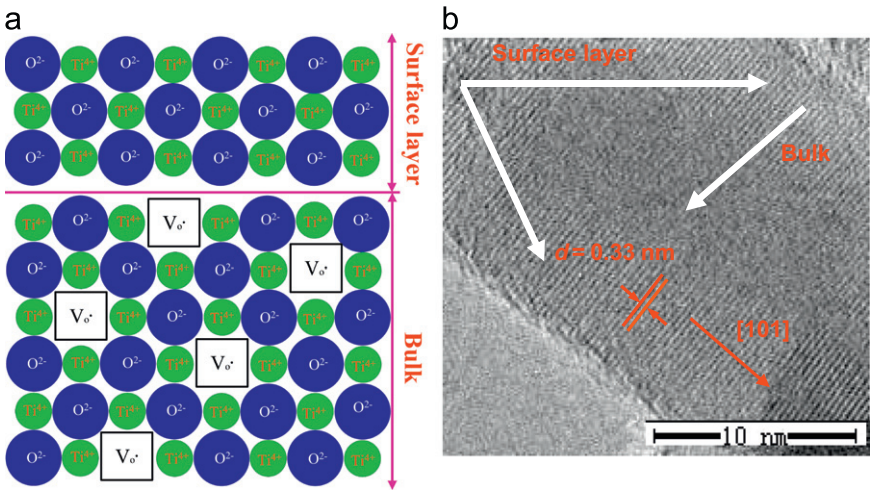

Fig. 7. (a) Schematic diagram for surface layer and bulk of novel TiO_2 (anatase) and (b) HRTEM image of novel TiO_2 (anatase).

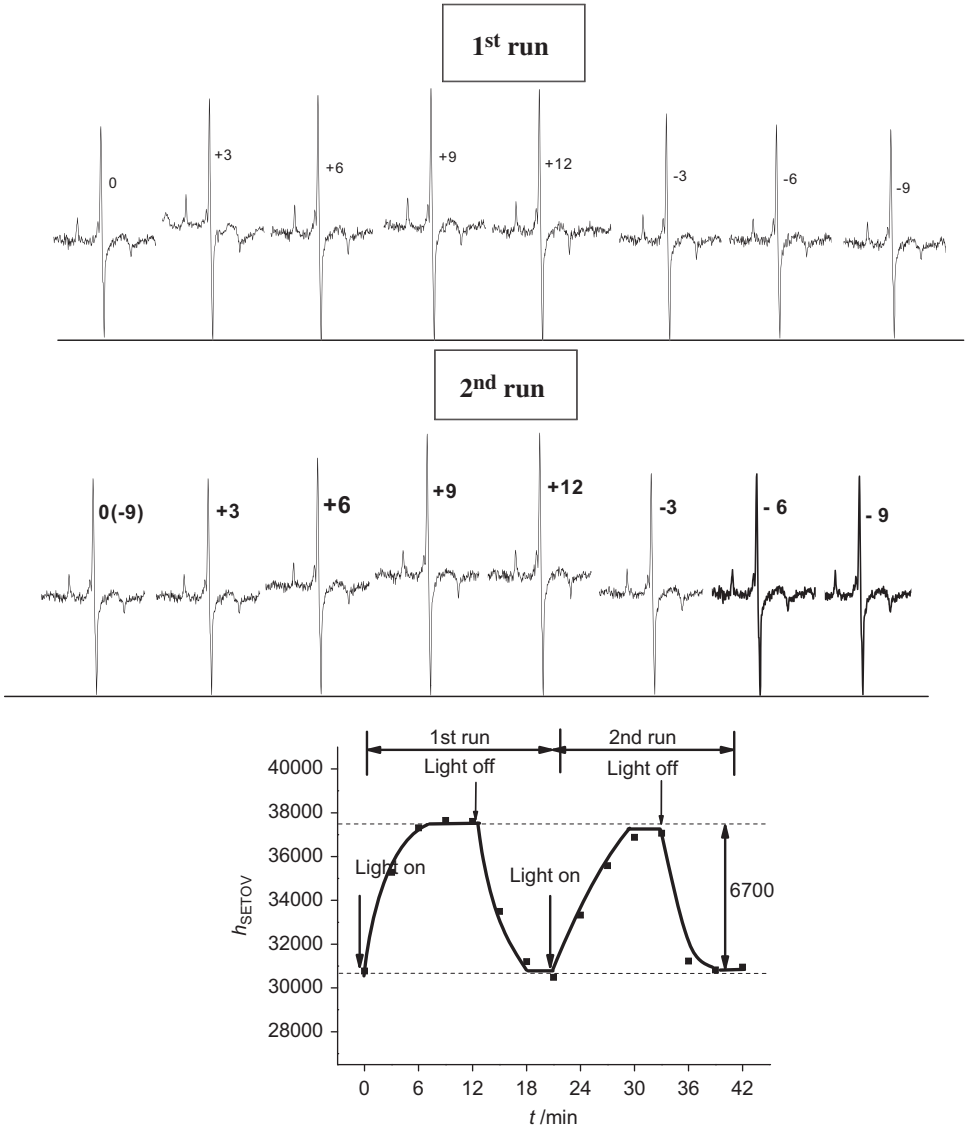

Fig. 8. Variation of ESR peak height h_{SETOV} with illumination time t.

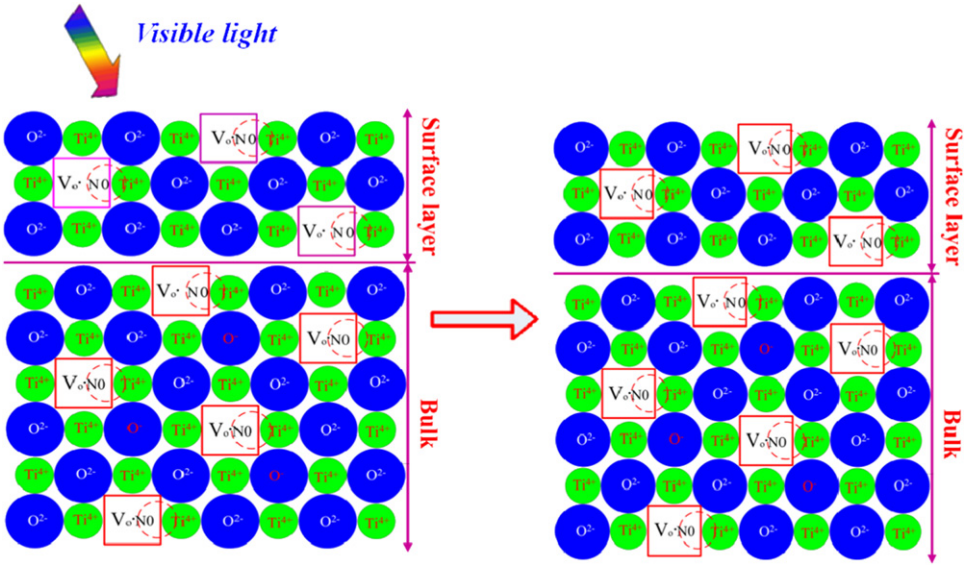

Scheme 2. Synergistic effect between $(V_o^{\bullet})_{bulk}$ and $(V_o^{\bullet})_{surf}$.

Secondly, active $(V_o^{\bullet\bullet})_{surf}$ can be generated on TiO_2 by treating in H_2 or in vacuum at elevated temperatures (formula 6), but the active $(V_o^{\bullet\bullet})_{surf}$ is instantly oxidized upon exposure to air (formula 7) [32,33]:

$$-Ti^{4+}-O-Ti^{4+}-+H_2 \rightarrow -Ti^{3+}-V_o^{\bullet\bullet}-Ti^{3+}-+H_2O \quad (6)$$

$$-Ti^{3+}-V_o^{\bullet\bullet}-Ti^{3+}-+1/2O_2 \rightarrow -Ti^{4+}-O-Ti^{4+}- \quad (7)$$

Then why $(V_o^{\bullet\bullet})_{surf}$ on the surface of N-doped novel TiO_2 (anatase) is stable in air? We suppose that NO could be chemisorbed at the adjacent sites of $(V_o^{\bullet\bullet})_{surf}$ and inhibit the attack of O_2 on $(V_o^{\bullet\bullet})_{surf}$ (see formula 7), resulting in significantly increased stability of $(V_o^{\bullet\bullet})_{surf}$ in air. This supposition is supported by relevant XPS result (see the inset in Fig. 3a; where N 1*s* XPS peak at a binding energy of 399.9 eV is assigned to N in NO [34–38] and corresponds to N atomic concentration of 1.0%). Synergistic action is realized between $(V_o^{\bullet})_{bulk}$ and $(V_o^{\bullet\bullet})_{surf}$ in the presence of active structures $(V_o^{\bullet})_{bulk}$–NO–Ti [22] and $(V_o^{\bullet\bullet})_{surf}$–NO–Ti (see Scheme 2).

4. Conclusions

(a) N-doped novel TiO_2 with desired visible light catalytic activity was prepared by calcinating novel TiO_2 (anatase) in flowing NH_3. N doping not only resulted in a high concentration of $(V_o^{\bullet})_{bulk}$–NO–Ti in resultant N-doped novel TiO_2 but also gave birth to $(V_o^{\bullet\bullet})_{surf}$. After N doping, NO was also chemisorbed on the vicinity of $(V_o^{\bullet\bullet})_{surf}$ and prevented the latter from being attacked by O_2, allowing $(V_o^{\bullet\bullet})_{surf}$ to remain stable in air. The stabilized $(V_o^{\bullet\bullet})_{surf}$ functioned as a surface electron trap and captured visible photogenerated electrons from the bulk, facilitating the redox reactions of propylene under visible light irradiation.

(b) Novel TiO_2 had response to visible light but did not contain electron traps on the surface, hence it did not possess visible photocatalytic activity. On the contrary, there existed synergistic effect between $(V_o^{\bullet})_{bulk}$–NO–Ti and $(V_o^{\bullet\bullet})_{surf}$–NO–Ti, the two kinds of active structures of N-doped novel TiO_2. This endowed N-doped novel TiO_2 with visible photocatalytic activity.

Acknowledgments

The authors are indebted to Prof. Chen Jingrong for her help in the measurements of and discussion on ESR data.

References

[1] R.C. Fang, Solid State Spectroscopy, Press of University of Science and Technology of China, Hefei, China, 2003 (in Chinese).
[2] S.C. Tsai, C.C. Kao, Y.W. Chung, J. Catal. 79 (1983) 451–461.
[3] A.L. Linsebigler, G.Q. Lu, J.T. Yates, Chem. Rev. 95 (1995) 735–758.
[4] A. Kudo, Y.G. Miseki, Chem. Soc. Rev. 38 (2009) 253–278.
[5] M. Su, Solid State Chemistry: An Introduction, Peking University Press, Beijing, China, 1987 (in Chinese).
[6] S.R. Morrison, The Chemical Physics of Surface, Plenum Press, New York, USA, 1977, pp. 184–188.
[7] W. Choi, A. Termin, M.R. Hoffman, J. Phys. Chem. 98 (1994) 13669–13679.
[8] M. Anpo, Catal. Surv. Jpn. 1 (1997) 169–179.
[9] D.C. Cronemeyer, Phys. Rev. 113 (1959) 1222–1226.
[10] E. Serwicka, M.W. Schlierkamp, R.N. Schindler, Z. Naturforch. 36a (1981) 226.
[11] E. Serwicka, Colloids Surf 13 (1985) 287–293.
[12] I. Nakamura, N. Negishi, S. Kutsuna, T. Ihara, S. Sugihara, K. Takeuchi, J. Mol. Catal. A: Chem 161 (2000) 205–212.
[13] R. Asahi, T. Morikawa, T. Ohwaki, K. Aoki, Y. Taga, Science 293 (2001) 269–271.
[14] R. Nakamura, T. Tanaka, Y. Nakato, J. Phys. Chem. B 108 (2004) 10617–10620.
[15] T. Lindgren, J.M. Mwabora, E. Avendano, J. Jonsson, C.G. Granqvist, S.E. Lindquist, J. Phys. Chem. A 107 (2003) 5709.
[16] S. Livraghi, M.C. Paganini, E. Giamello, A. Selloni, C.D. Valentin, G. Pacchioni, J. Am. Chem. Soc. 128 (2006) 15666–15671.
[17] N. Serpone, J. Phys. Chem. B 110 (2006) 24287–24293.
[18] V.N. Kuznetsov, N. Serpone, J. Phys. Chem. B 110 (2006) 25203–25209.
[19] A.V. Emeline, N.V. Sheremetyeva, N.V. Khomchenko, V.K. Ryabchuk, N. Serpone, J. Phys. Chem. C 111 (2007) 11456–11462.
[20] Y. Wang, C.X. Feng, Z.S. Jin, J.W. Zhang, J.J. Yang, S.L. Zhang, J. Mol. Catal. A: Chem 260 (2006) 1–3.
[21] Y. Wang, J.W. Zhang, Z.S. Jin, Z.S. Wu, S.L. Zhang, Chin. Sci. Bull. 52 (2007) 1973–1976.
[22] C.X. Feng, Y. Wang, Z.S. Jin, J.W. Zhang, S.L. Zhang, Z.S. Wu, Z.J. Zhang, New J. Chem. 32 (2008) 1038–1047.
[23] J.W. Zhang, Y. Wang, Z.S. Jin, Z.S. Wu, Z.J. Zhang, Appl. Surf. Sci. 254 (2008) 4462–4466.
[24] M. Zhang, Z.S. Jin, J.W. Zhang, X.Y. Guo, J.J. Yang, W. Li, X.D. Wang, Z.J. Zhang, J. Mol. Catal. A: Chem. 217 (2004) 203–210.
[25] Q.Y. Li, J.W. Zhang, Z.S. Jin, D.G. Yang, X.D. Wang, J.J. Yang, Z.J. Zhang, Electrochem. Commun. 8 (2006) 741–746.
[26] Q.Y. Li, X.D. Wang, Z.S. Jin, D.G. Yang, S.L. Zhang, X.Y. Guo, J.J. Yang, Z.J. Zhang, J. Nanopart. Res. 9 (2007) 951–957.
[27] L. Qian, Z.S. Jin, J.W. Zhang, Y.B. Huang, Z.J. Zhang, Z.L. Du, Appl. Phys. A 80 (2005) 1801–1805.
[28] X.D. Wang, Z.S. Jin, Z.J. Zhang, Prog. Chem. 18 (2006) 1208–1217 (in Chinese).

[29] J.J. Yang, Z.S. Jin, X.D. Wang, W. Li, J.W. Zhang, S.L. Zhang, X.Y. Guo, Z.J. Zhang, Dalton Trans. (2003) 3898–3901.
[30] S.L. Zhang, W. Li, Z.S. Jin, J.J. Yang, J.W. Zhang, Z.L. Du, Z.J. Zhang, J. Solid State Chem. 177 (2004) 1365–1371.
[31] W. Li, Z.S. Jin, J.J. Yang, Z.J. Zhang, Ima. Sci. Photochem. 21 (2003) 273–279 (in Chinese).
[32] T. Ihara, Y. Ikeuchi, M. Miyoshi, M. Ando, S. Sugihara, Y. Iriyama, J. Mater. Sci. 36 (2001) 4201.
[33] K. Takeuchi, I. Nakamura, O. Matsumoto, S. Sugihara, M. Ando, T. Ihara, Chem. Lett. 29 (2000) 1354–1355.
[34] C. Burda, Y. Lou, X. Chen, A.C.S. Samia, J. Stout, J.L. Gole, Nano Lett. 3 (2003) 1049–1051.
[35] J.L. Gole, J.D. Stout, C. Burda, Y. Lou, X. Chen, J. Phys. Chem. B 108 (2004) 1230–1240.
[36] X. Chen, Y. Lou, A.C.S. Samia, C. Burda, J.L. Gole, Adv. Funct. Mater. 15 (2005) 41–49.
[37] S.M. Prokes, J.L. Gole, X. Chen, C. Burda, W.E. Carlos, Adv. Funct. Mater. 15 (2005) 161–167.
[38] J.A. Rodriguez, T. Jirsak, J. Dvorak, S. Sambasivan, D. Fischer, J. Phys. Chem. B 104 (2000) 319–328.